

# INTERPRETATION OF THE DATA OF EPSILON AURIGAE

Shusaku Kawabata  
Kyoto Gakuen University  
Sogabe-machi, Kameoka, Kyoto  
Japan

## 1. INTRODUCTION

Various interpretations of the data of Epsilon Aurigae had been proposed before the recent eclipse. Every model explains the observations to a certain extent, but simultaneously disagrees with some other aspects of the nature of this system. During the 1982-84 eclipse, observations extending from far UV to IR have been carried out. A lot of data have been obtained and discussed in the workshop held at Arizona on this January. The spectroscopy and the photometry in visual region, however, are still important particularly to get informations about dynamical features of the components. In this review we present several interpretations mainly using new data obtained from ground-based spectroscopic observations including ours.

## 2. NATURES OF COMPONENTS

### 2.1. Opacity Source of Eclipse

Kuiper et al. (1937) assumed electron scattering as the cause of wavelength independence of eclipse depth. From analysis of several Mt. Wilson plates obtained during 1955-57 eclipse Hack (1958) derived the high electron density enough to produce eclipse extinction by electron scattering and considered a high temperature object in the center of the secondary as the ionization source. Excess radiation shorter than 1400Å found by IUE (Hack and Selvelli 1979; Boehm et al. 1984; Parthasarathy and Lambert 1984) may be candidate of hot B star, but Ake and Simon (1984) show spectrum of that region does not match with B type star.

Kopal (1954) proposed a dust ring surrounding the secondary component as the alternative cause of the opacity during eclipse. From recent IUE observations Chapman et al. (1983) considered absorption by dust shortward of 3000Å. Boehm et al. (1984) pointed out that the secondary's disk should not be made of standard composition of dust because of the absence of deepening of the 2200Å absorption, and Ake and Simon (1984) suggested composition with larger grains. Backman et al. (1984) found IR excess radiation and identified the secondary as a source of emission

with  $T=500\text{K}$ . They derived the results under the constancy of eclipse depth from  $0.4$  to  $10\ \mu\text{m}$  and dusty cloud structure of the secondary. Their results may give a clue to the problem of the opacity source.

## 2.2. Scattered Light

Radial velocities during eclipse were measured by Struve et al. (1958) and Wright (1970) for 1955–57 eclipse and by Ferluga and Hack (1958) and by us (Saito, Kawabata, Saijo and Sato 1984, 1985) for this eclipse. Additional lines during eclipse, considered to be due to absorption of the secondary atmosphere, make measurements complicated. Struve et al. (1958) found differential velocity shift, namely larger radial velocity for stronger intensity of line in ingress and reverse for egress. Direct measurements of our spectrograms obtained in the 1982–84 eclipse show the same trend as Struve et al.'s (figure 1). To extract changes of spectra in eclipse we divide intensities of spectra in eclipse by reference spectrum taken outside eclipse and normalize at continuum part. Resultant profiles change from inverse P-Cygni type before mideclipse to P-Cygni type after mideclipse (figure 2). Intensities of the emission features of profiles do not depend on those of absorption features, but are proportional to the intensities of reference lines. Plotting the excess intensity  $y$  of emission features against reciprocal of the residual intensity  $I_{0,c}/I_{0,\lambda}$  of reference line (figure 3) we obtain

$$y = 1 + a(I_{0,c}/I_{0,\lambda} - 1) \quad (1)$$

where  $a$  is a constant. The light observed in eclipse contains the light scattered by dust and gas. Then it turns out that  $a$  represents fraction of scattered light in the total light in eclipse:

$$a = \frac{I_{\text{scat}}}{(I_0/S) \int \exp(-\tau_c) dS + I_{\text{scat}}} \quad (2)$$

where  $I_0$  is the intrinsic intensity of the primary,  $I_{\text{scat}}$  is that of the scattered light, and  $S$  is the cross section of the primary. We found that  $a$  ranges  $1/3 \sim 1/5$ . Removing scattered light, we obtain line profiles due to absorption of secondary gas. Apparent differential velocity shift disappears in the resulting profiles, and the velocities correspond to larger values in absolute magnitude shown in figure 1.

## 2.3. Rotation Feature of the Secondary

Change of radial velocities of metallic lines, Balmer lines, and satellite lines of CaII H and K shows that (1) secondary's gas rotates around the center, (2) velocity separation among the elements occur in inner phase and (3) velocities in absolute value differ between ingress and egress sides though orbital velocity of the primary is nearly equal to zero at mideclipse (figure 4). Our velocities almost agree with those by Ferluga and Hack (1985). We calculated profiles of metallic

lines assuming the structure of the secondary's disk which shall be described later. Resulting absorption profiles around the second and the third contacts show that the radial velocities at the bottom of line profiles are about 0.8 ~ 0.95 times the rotation velocity at limb. The observed values of radial velocities yield the rotation velocity of 37 ~ 42 km s<sup>-1</sup> at the ingress side limb and 41 ~ 43 km s<sup>-1</sup> at the egress side limb of the disk.

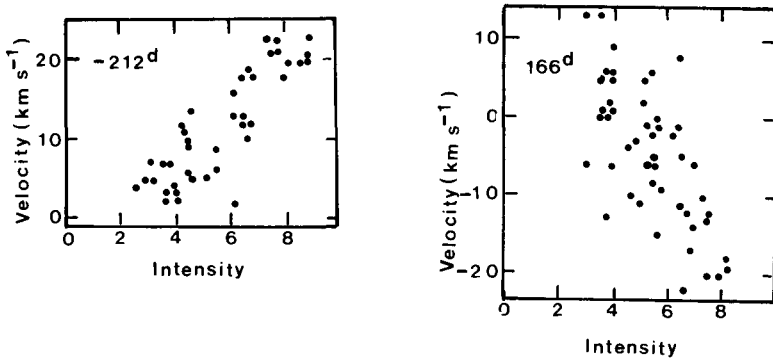


Fig.1. Radial velocities of the absorption lines against the line intensities.

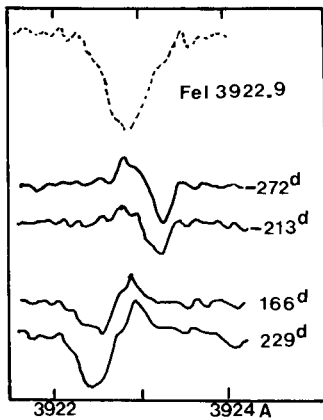


Fig.2. An example of absorption profile due to secondary. The top is the reference spectra in twice scale of the intensity.

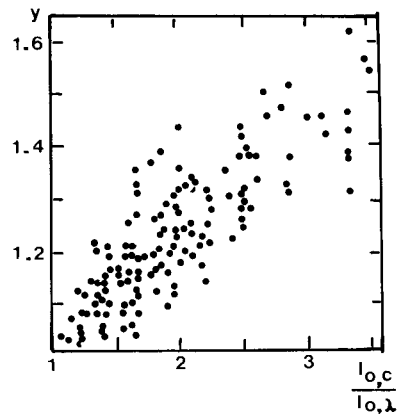


Fig.3. Intensity y of emission features against that of reference line (near second contact).

Observations of  $H\alpha$  line have been done at several observatories. Variation of the profile with eclipse phase is similar to that found for the 1955-57 eclipse by Wright and Kushwaha (1958). Absorption profiles of  $H\alpha$  due to the secondary consist of three features; i.e., (1) broad absorption with center at nearly zero velocity appearing from phase before the first contact to phase after the fourth contact, (2) absorption moving from red side at ingress to violet side at egress, and (3) broad wing near mideclipse, as is shown in figure 5. These features originate respectively from vastly extended gas, the extended rotating gas, and rapidly rotating gas just around the secondary's center. It has been found that calculated profiles in the case of Keplerian rotation with rotational velocity at limb of  $38 \sim 40 \text{ km s}^{-1}$  coincide with observational profiles.

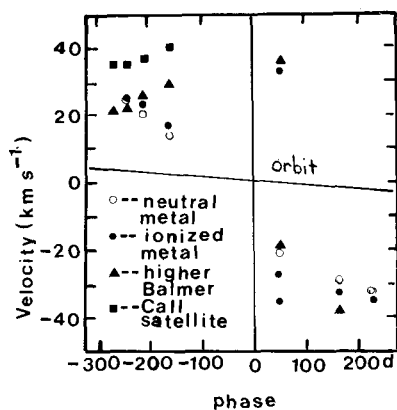


Fig. 4. Radial velocities of the secondary gas against the eclipse phase.

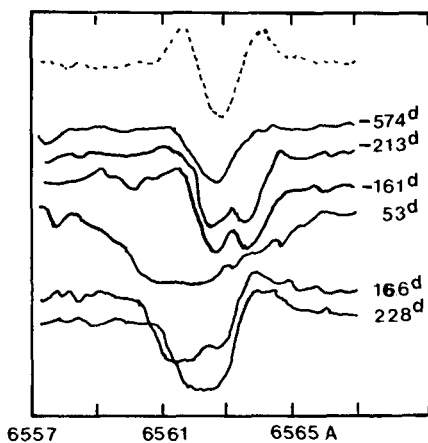


Fig. 5. Variation of  $H\alpha$  absorption due to the secondary. The top is the reference spectra in twice scale of the intensity.

#### 2.4. Ring Structure of the Secondary

We obtained curves of growth of FeI, FeII, and TiII for phases -211d, 166d, and 229d. Comparison of column densities of elements at 229d are higher than those at 166d, suggesting ring structure of the secondary disk. As is seen from figure 4, the velocities of neutral and ionized metallic lines decrease almost linearly with eclipse phase. This phenomena also indicates a ring like distribution of the elements.

Huang (1965) presented a model of completely opaque disk seen edge on. Wilson (1971) considered dust ring with a semitransparent central opening. From photometric contact times (e.g., Ohki and Sakai 1985; Schmidtke 1985; JAPOA 1983) and growth and decay of broad wings of the lower Balmer lines, we have estimated the radius  $R_1$  of the primary and

the length  $l_2$  of the secondary disk as

$$R_1 = 0.87(1 + m_1/m_2) \text{ AU} \quad (3)$$

and

$$l_2 = 5.5(1 + m_1/m_2) \text{ AU} \quad (4)$$

The density distributes in the secondary's isothermal Keplerian disk as

$$\rho(r, z) = \rho_0(r) \exp \left\{ - \left[ \frac{v(r)}{c_s} \right]^2 \left[ 1 + \left( \frac{z}{c_s} \right)^2 \right]^{-\frac{1}{2}} - 1 \right\} \quad (5)$$

where  $r$  and  $z$  are respectively the radial and vertical distances of the cylindrical coordinate whose origin is at the rotation center.  $v(r)$  is the rotation velocity in the plane of  $z=0$ , and  $c_s$  is speed of sound. Taking into account of such dimensions and the density distribution we calculated light curve and the line profiles whose results have been mentioned above. A ring structure of the dust distribution is required to satisfy both central brightening of the eclipse light curve and the appearance of the high velocity wings in the lower Balmer lines near mideclipse: e.g.,  $\rho(r)=\text{const.}$  at  $0.5 < r < 1$  and zero at  $0 < r < 0.5$  with  $c_s/v_{\text{rot}} = 0.1$ , where  $r$  is in unit of the radius of the disk and  $v_{\text{rot}}$  is the rotation velocity at the limb of  $z=0$ .

### 2.5. Asymmetric and Inhomogenous Features of the Secondary Disk

The width of the  $H\alpha$  line changes with phase indicating a maximum at a phase 20 days after the mideclipse. This implies that center of mass of the secondary deviates from the apparent center of the secondary.

Excitation temperatures obtained from curves of growth are found to be 4000K - 4700K for TiIII and FeI, but FeII shows 8900K in ingress side. As mentioned above, the radial velocities at ingress side are about  $10 \text{ km s}^{-1}$  less than the velocities in absolute magnitude at egress side. These two features are explained as the result of the formation of shock front at ingress side of the secondary disk. The shock originates as well as an ionization front by the UV radiation from the primary. Excess Lyman photon flux can be expected from observations by the IUE (Parthasarathy and Lambert 1984).

### 2.6. $H\alpha$ Emitting Region of the Primary

The calculated profiles of  $H\alpha$  line fit to the observed ones when the length of  $H\alpha$  emitting region of the primary along the secondary's disk is slightly larger than the primary's photosphere and the length along the vertical direction is 0.2 times as large as the photosphere. Kemp et al. (1985) proposed from the observation of polarization that there is an equatorial chromospheric belt of the primary.  $H\alpha$  emitting region may corresponds to this belt.

## 3. MASSES AND LUMINOSITIES OF THE COMPONENTS

Traditionally accepted values of masses of the primary and the secondary

are  $m_1 \approx 15M_{\odot}$  and  $m_2 \approx 13M_{\odot}$  by Morris (1965), based on theoretical model of Hayashi and Cameron (1962). Backman et al. (1984) found the solid angle subtended by the secondary to be  $8 \cdot 10^{-16}$  ster which has been confirmed by data of IRAS (Backman and Gillet 1985). For the distance of 580 pc by van de Kamp (1978) and 0.84 of interstellar absorption,  $M_V$  becomes  $-6.7$ , i.e.,  $L_1 = 10^{4.6} L_{\odot}$ . Backman et al. (1984) obtained  $L_2 = 10^2 L_{\odot}$  from their observation.

From the mass function and Keplerian motion in the secondary's disk we have

$$1 + m_1/m_2 = 0.19 \sin i (1-e)^{-2} K_1^{-2} v_{\text{rot}}^2 \quad (6)$$

and

$$m_2 = 3.6 \cdot 10^{-5} \sin^2 i (1-e)^{-5/4} K_1^{-1} v_{\text{rot}}^4 M_{\odot}, \quad (7)$$

where  $i$ ,  $e$ , and  $K_1$  are the inclination, the eccentricity, and the velocity amplitude in  $\text{km s}^{-1}$ , and  $v_{\text{rot}}$  is also in  $\text{km s}^{-1}$ . We obtain  $m_1$  and  $m_2$  with our observed value of  $v_{\text{rot}}$ . Adopting values of  $i = 80^{\circ} \sim 90^{\circ}$ ,  $e = 0.0 \sim 0.2$ ,  $K_1 = 15 \sim 17 \text{ km s}^{-1}$ , and  $v_{\text{rot}} = 38 \sim 42 \text{ km s}^{-1}$ , suitable values become  $m_1 = 1.5 \sim 2.7 M_{\odot}$ ,  $L_1 = 10^{5.0} \sim 10^{5.1} L_{\odot}$ ,  $m_2 = 6.5 \sim 7.6 M_{\odot}$ , and  $L_2 = 10^{2.6} \sim 10^{2.9} L_{\odot}$ . The value of  $L_1$  is nearly equal to Eddington limit.

Such results for masses differ considerably from usually believed values. Models with secondary component which is itself a binary have been presented by Lissauer and Backman (1984) and Eggleton and Pringle (1985). The former is premised on massive system, while the latter considers  $1.3M_{\odot}$  primary of contracting phase after Roche lobe filling. Takeuti (1986) has pointed out that  $1M_{\odot}$  primary is consistent with the observed period of the Cepheid-like pulsation. Webbink (1985) has examined possible evolutionary phase in which a member of binary passes through an F0 supergiant stage and has shown possibility of pre-white dwarf stage of the primary with  $1M_{\odot}$  combined with the secondary of  $4.8M_{\odot}$ . He considers the stage is more successful to account for large luminosity difference of components. Estimation of masses of components is one of fundamental problems for the interpretation of data of Epsilon Aurigae.

#### 4. FINAL REMARKS

We summarized several points of interpretation of data from mainly ground-based spectroscopy, but there remain many important problems to be investigated: for example, as for the secondary's disk, the multiplicity of the temperature, the source of the continuous absorption, the formation and the stability of the disk, and so on. The nature of the central object of the secondary is almost enigmatic yet. We have presented peculiar characteristics of the primary now. Recently Saito and Kitamura (1985) suggest a violent collapse of the atmosphere of the primary from the analysis of radial velocities of outside eclipse. Studies from the viewpoint of the evolutionary situation of binary system and further successive observations are desirable about various item to unveil these puzzling components.

## REFERENCES

- Ake, T.B., and Simon, T. 1984, NASA Publ. No.2349, p.361.
- Backman, D.E., and Gillet, F.C. 1985, submitted to Astrophys. J.
- Backman, D.E., Becklin, E.E., Cruikshank, D.P., Joice, R.R., Simon, T., and Tokunaga, A. 1984, Astrophys. J., 284, 799.
- Boehm, C., Ferluga, S., and Hack, M. 1984, Astron. Astrophys. 130, 419.
- Chapman, R.D., Kondo, Y., and Stencel, R.E., 1983, Astrophys. J. Lett., 269, L17.
- Eggleton, P.P., and Pringle, J.E., 1985, Astrophys. J., 288, 275.
- Ferluga, S., and Hack, M. 1985, in Proceedings of North American Workshop on the Recent Eclipse of Epsilon Aurigae, ed. R.E. Stencel.
- Hack, M. 1985, Astrophys. J., 128, 287.
- Hack, M., and Selvelli, P.L. 1979, Astron. Astrophys. 75, 316.
- Hayashi, C., and Cameron, R.C., 1962, Astrophys. J., 136, 166.
- Huang, S.S. 1965, Astrophys. J., 141, 976.
- JAPOA (Japan Amateur Photoelectric Observers Association) 1983, Inf. Bull. Var. Stars, I.A.U. No2371.
- Kemp, J.C., Henson, G.D., Krau, D.J., and Beardsley, I.S. 1985, in Proceedings of North American Workshop on the Recent Eclipse of Epsilon Aurigae, ed. R.E. Stencel.
- Kopal, Z. 1954, The Observatory, 74, 14.
- Kuiper, G.P., Struve, O., and Strömgren, B. 1937, Astrophys. J., 86, 570.
- Lissauer, J.J., and Backman, D.E. 1984, Astrophys. J. Lett., 286, L39.
- Morris, S.C. 1965, Astron. J., 70, 685.
- Ohki, T., and Sakai, Y. 1985, submitted to Sci. Rep. Fukushima Univ.
- Parthasarathy, M., and Lambert, D.L. 1983, Publ. Astron. Soc. Pacific, 95, 1012.
- Saito, M., Kawabata, S., Saijo, K., and Sato, H. 1984, Astrophys. Space Sci., 99, 269.
- Saito, M., Kawabata, S., Saijo, K., and Sato, H. 1985, submitted to Publ. Astron. Soc. Japan.
- Saito, M., and Kitamura, M. 1985, submitted to Astrophys. Space Sci.
- Schmidtke, P.C. 1985, Eps. Aur. Campaign Newsletter, No.13, p.17.
- Stencel, R.E. 1985, Proceedings of North American Workshop on the Recent Eclipse of Epsilon Aurigae.
- Struve, O., Pillans, H., and Zebergs, V. 1958, Astrophys. J., 128, 287
- Takeuti, M. 1986, Astrophys. Space Sci. 120, 1.
- van de Kamp, P. 1978, Astron. J., 83, 975.
- Webbink, R.F. 1985, in Proceedings of North American Workshop on the Recent Eclipse of Epsilon Aurigae.
- Wilson, R.E. 1971, Astrophys. J., 170, 529.
- Wright, K.O. 1970, Vistas Astron., 12, 147.
- Wright, K.O., and Kushwaha, R.S. 1957, Comm. Coll. Intern. Astrophys. Liege, 8, 421.